5-aminoisoquinoline improves renal function and fibrosis during recovery phase of cisplatin-induced acute kidney injury in rats

Andrés Quesada,[1] Francisco O'Valle,[2,3,6] Sebastián Montoro-Molina,[1] Mercedes Gómez-Morales,[2] Mercedes Caba-Molina,[2] Juan Francisco González,[2] María C. de Gracia[4], Antonio Osuna,[4] Félix Vargas,[5,6] Rosemary Wangensteen.[1]

[1]Área de Fisiología, Departamento de Ciencias de la Salud, Universidad de Jaén, Jaén, Spain

[2]Departamento de Anatomía Patológica, Facultad de Medicina, Universidad de Granada,

[3]Instituto de Biomedicina y Medicina Regenerativa (IBIMER), Granada, Spain

[4]Unidad de Nefrología, FIBAO, Hospital Virgen de las Nieves, Granada, Spain

[5]Departamento de Fisiología, Facultad de Medicina, Universidad de Granada, Granada, Spain

[6]Instituto Biosanitario de Granada (IBS), Granada, Spain

Running title: Effect of 5-AIQ in cisplatin-treated rats

Keywords: 5-aminoisoquinoline, cisplatin, renal fibrosis.

Wordcount: 5197.

Correspondence to: Rosemary Wangensteen, PhD; Desp. 244, Edf. B-3; Campus Las Lagunillas; Universidad de Jaén; 23071, Jaén, Spain; Phone: 34953212407; Fax: 34953212943; e-mail: rwangens@ujaen.es

Abstract

The aim of this study is to analyze the effects of 5-aminoisoquinoline (5-AIQ), a poly(ADP-ribose) polymerase-1 (PARP1) inhibitor, over renal dysfunction and fibrosis during recovery phase of cisplatin-induced acute kidney injury (AKI) in rats. Male Wistar rats were distributed in three groups (n=8 each group): control, cisplatin (CisPt) and CisPt+5-AIQ. Control and CisPt groups received a subcutaneous injection of either saline or 7 mg/kg cisplatin, respectively. CisPt+5-AIQ group received two intraperitoneal injections of 10 mg/kg 5-AIQ 2 hours before and 24 hours after cisplatin treatment. 13 days after treatment, rats were housed in metabolic cages and 24-h urine collection was made. At day 14, cisplatin-treated rats showed increased diuresis, N-acetyl-β-D-glucosaminidase (NAG) excretion, glucosuria and sodium fractional excretion, and decreased creatinine clearance (CrCl). 5-AIQ significantly increased CrCl and decreased NAG excretion, glucosuria and sodium fractional excretion. In plasma, cisplatin increased sodium, urea and creatinine concentration, while 5-AIQ treatment decreased these variables to the levels of control group. 5-AIQ completely prevented the body weight loss evoked by cisplatin treatment. Cisplatin also induced an increased renal expression of PAR polymer, α-smooth muscle actin (α-SMA), transforming growth factor-β1 (TGF-β1) and collagen-IV. These variables were decreased in CisPt+5-AIQ group. Tubular lesions and renal fibrosis were also decreased by 5-AIQ treatment. We conclude that inhibition of PARP1 with 5-AIQ can attenuate long-term nephrotoxic effects associated with cisplatin treatment, preventing renal dysfunction and body weight decrease, and ameliorating tubular lesions and collagen deposition.

Introduction

Cisplatin (CisPt) is an antitumoral agent that induces direct proximal tubular nephrotoxicity in both humans and animals [1,2]. This side effect limits the use of CisPt, because one-third of the patients develop renal dysfunction after CisPt treatment [3-5]. Although the mechanisms implicated in CisPt nephrotoxicity are not completely elucidated, it has been published that poly(ADP-ribose) polymerase 1 (PARP1) is an important mediator of CisPt-induced renal tubular necrosis and inflammation [6,7].

PARP1 is a nuclear enzyme that repairs DNA strands in homeostatic conditions, converting NAD^+ in ADP-ribose. Nevertheless, its overactivation in several pathological conditions induces a depletion of NAD^+ and ATP that triggers to cellular death and up-regulation of key inflammatory pathways [8,9].

Inhibitors of PARP1 alone or in combination with DNA-damaging anticancer agents have been proved to facilitate tumor cell death [10-14] and it has been demonstrated a synergistic chemosensitivity with cisplatin in breast cancer cell lines [15]. Therefore, inhibition of PARP1 in CisPt treatment can be of great interest since it could potentiate antitumoral effects of CisPt. Moreover, pharmacologic inhibition or genetic deletion of PARP1 also attenuated CisPt-induced increased oxidative and nitrative stress [16] that has been involved in cisplatin-induced renal interstitial fibrosis [17].

These previous reports seem to indicate that PARP1 plays a role in cisplatin-associated nephrotoxicity. Thus, inhibitors of PARP1 have been demonstrated to improve short-term renal dysfunction in cisplatin-treated mice [7,16], but the effects of PARP1 inhibition over long-term renal dysfunction and fibrosis that are associated to cisplatin treatment have not been studied. Therefore, the aim of this work was to study if the inhibition of PARP1 with 5-aminoisoquinoline (5-AIQ) prevented long-term CisPt-

associated nephrotoxicity, analyzing the effects of this treatment over renal function and histopathological lesions, focusing our attention on the mechanisms underlying renal fibrosis in this model. To do it, we analyzed renal expression of α-smooth muscle actin (α-SMA), as an index of myofibroblast activation, transforming growth factor-β1 (TGF-β1) as mediator of interstitial fibrosis [18], and collagen-IV deposition.

Materials and methods

Ethical approval

All experimental procedures were performed according to the European Union Guidelines to the Care and Use of Laboratory Animals and approved by the Ethical Committee of the University of Jaén.

Animals and drugs

24 male Wistar rats weighing 242 ± 6.69 g were purchased from Harlan Laboratories (Barcelona, Spain). These rats were kept in a room maintained at 24±1°C and humidity of 55±10%, with a 12-h light/dark cycle and had free access to rat chow and tap water. Cisplatin and 5-AIQ were purchased from Sigma-Aldrich (Darmstadt, Germany).

Experimental protocols

Rats were distributed in three groups: Control, CisPt and CisPt+5-AIQ (n = 8 each group). Control and CisPt groups received a subcutaneous injection of either saline or 7 mg/kg of cisplatin, respectively. Cispt was dissolved in saline at a concentration of 0.35 mg/ml under sonication. CisPt+5-AIQ group received two i.p. injection of 10 mg/kg of 5-AIQ dissolved in saline 2 hours before and 24 hours after CisPt treatment. Volumes of injections were calculated regarding to the weight of each animal. Control and CisPt

groups were also injected with the same proportional volume of saline. 13 days after CisPt or saline administration, rats were housed in metabolic cages and 24-h urine collection was made. Urine samples were centrifuged 15 min at 1000 *g* and frozen at -80 ºC until assay. Blood samples were obtained from left ventricle under anesthesia (pentobarbital, 50 mg/kg, i.p.), centrifuged 15 min at 1000 *g*, and stored at -80 ºC. Kidneys were removed and weighted. One kidney was fixed in 10% neutral-buffered formaldehyde solution during 48 h and subsequently placed in 70% ethanol for histological studies.

Analytical procedures

Proteinuria, urine creatinine and N-acetyl-β-*D*-glucosaminidase (NAG) were determined in urine samples with an autoanalyzer Spin120. Plasma creatinine and urea were also measured in this instrument. Reagents for proteinuria (ref. MI1001025), urea (ref. MI41041) and creatinine-Jaffé method (ref. MI1001111) were provided by Spinreact (Barcelona, Spain). Reagent for NAG was purchased to Dyazyme Laboratories (Poway, CA, USA) (ref. DZ062A-K).

Plasma and urinary sodium were quantified with a sodium selective electrode in an EasyElectrolyte instrument (Medica Corporation, Bedford, MA, USA).

Renal expression of PAR polymer was measured to evaluate the ability of 5-AIQ to inhibit PARP1 using indirect ELISA. α-Smooth muscle actin (α-SMA), transforming growth factor-β1 (TGF-β1) and collagen-IV were also measured in renal tissue by indirect ELISA. Tissues were homogenized in pH 7.4 50 mM HCl-Tris and centrifuged for 15 min at 1000g. 50 µl of supernatants containing 10 µg/ml of protein were fixed in a 96-well plate (Nunc Maxisorp, VWR International Eurolab, Barcelona, Spain) overnight at 4º C. After blocking with 100 µl of PBS containing 5% of albumin during 2

hours at room temperature, the plate was probed overnight at 4ºC with 50 µl of 1 µg/ml of rabbit anti-PAR (Trevigen, Gaithersburg, MD, USA), anti α-SMA (Proteintech, Manchester, UK), anti- collagen-IV (Proteintech, Manchester, UK) or anti- TGF-β1 as primary antibodies, and 1 hour at 37 ºC with 50 µl of 0.2 µg/ml of mouse anti-rabbit horseradish peroxidase-linked IgG antibody (KPL Inc., Gaithersburg, MD, USA) as secondary antibody. Plate was washed after blocking and after each antibody incubation with 250 µl of pH 7.4 50 mM Tris containing 0.05 % Tween-20 during 3 minutes for 5 times. After washing, plate was incubated with 50 µl of 3, 3', 5, 5'-tetramethylbenzidine (TMB) for 30 minutes at 37 ºC, and reaction was stopped by adding 50 µl of HCl 1 N. Absorbance was read at a wavelength of 450 nm with a reference wavelength of 590 nm. All samples were analyzed in duplicate. Results were expressed as percentage of the mean absorbance of the control group. Tissue protein was determined with the DC Protein Assay kit (Bio-Rad, Hercules, CA, USA).

Histopathological analysis

For conventional morphology, the kidneys were buffered 10% formaldehyde-fixed, during 48 h at room temperature, dehydrated and paraffin-embedded in an authomatic tissue processor (Thermo Scientific Excelsior AS, Thermo Fisher Scientific, Waltham, Massachusetts, USA), and transversal sections in horizontal plane were deparaffinized in xylol (3 passes of 5 minutes) and re-hydrated in ethanol of decreasing gradation (absolute, 96%, and 70%, 2 passes of 3 min, respectively). Kidneys sections were stained with hematoxylin and eosin, Masson's trichrome and periodic acid-Schiff stain (PAS). The morphological study was done in blinded fashion on 4-micrometer sections with BX42 light microscopy (Olympus Optical Company, Ltd., Tokyo, Japan), using the most appropriate stain for each lesion (S3 dysplasia, acute tubular necrosis,

apoptosis, casts, tubular atrophy, tubular dilation, vacuolization, inflammatory infiltrate, tubular mitosis). The severity of lesions was calculated semiquantitatively using a 0 to 3 scale (0, absence; 1, mild [<10% of juxtamedullary proximal tubules, vessels or glomeruli involved]; 2, moderate [10 to 25%]; 3, severe [>25%]).

Morphometrical analysis

Kidney samples fixed in buffered 10% formalin were embedded in paraffin and serially sectioned at 5 µm thickness. Afterwards, they were stained with 1% picro Sirius red F3BA (Gurr, BDH Chemicals Ltd., Poole, United Kingdom) for image analysis quantification. To improve staining, tissue sections were kept after deparaffination for 3-5 days in 70% ethanol as mordent. Picro Sirius red stains connective fibers deep red and cell nuclei and cytoplasmatic structures light red/bright yellow [19]. 20 images of corticomedullary junction per kidney were acquired using an IF 550 green optical filter with illumination intensity values slightly above those used for normal observation with a digital camera 3CCD (DP70) coupled to an Olympus BX-42 microscope. (Olympus Optical Company). 20 images of corticomedullary junction per kidney were acquired using polarized light. Histologic images of kidney biopsies were convert in black and white at 8 bit intensity resolution (256 gray levels) with a global magnification of 200X, and normalized with Adobe Photoshop software (Adobe Systems Software, Ireland). To assess the fibrosis, we made a macro that included a semiautomatic thresholding of the total of the images per group of rats simultaneously with Image J software (National Institute of Health, USA).

Statistical analysis

StatGraphics software was used for statistical analysis. One-way ANOVA and Bonferroni's test were used for the analysis of variables with normal distribution. Mann-Whitney W

(Wilcoxon) test was used to analyze the differences in tubular lesions. A *p*-value of 0.05 was accepted for statistical significance threshold.

Regression analysis was made with StatGraphics software, selecting a linear model to correlate NaFE and CrCl in Control and CisPt+5-AIQ groups, and a multiplicative model in CisPt group.

Results

Morphologic and metabolic variables

Treatment with CisPt evoked a progressive loss of body mass along the two weeks of experiment, and also increased kidney weight in comparison with control animals. Both morphologic alterations were prevented by treatment with 5-AIQ (Table 1).

Water intake and diuresis were increased in CisPt treated rats and remained increased in CisPt+5-AIQ group 14 days after CisPt injection. Nevertheless, water balance was similar in control and CisPt groups, and treatment with 5-AIQ induced a significant increase in this variable.

Renal function studies

Fig. 1 shows that CisPt treatment decreased creatinine clearance (CrCl) 14 days after CisPt injection. Inhibition of PARP1 with 5-AIQ evoked an increase of CrCl in CisPt-treated rats, and no significant differences were found between CisPt+5-AIQ and control group. In plasma, CisPt group displayed higher concentrations of urea and creatinine that were also reduced at the level of control group with 5-AIQ treatment.

Regarding to urinary variables, cisplatin augmented NAG excretion and glucosuria (Table 2). 5-AIQ treatment significantly decreased NAG excretion and glucosuria in

comparison with CisPt-treated group. Proteinuria was similar in all experimental groups (Table 2).

Sodium handling

Treatment with CisPt increased plasma sodium concentration, and 5-AIQ reduced this variable to the level of control group (Table 3) 14 days after CisPt injection.

Despite the increased plasma sodium, sodium tubular load (NaTL), parameter that quantify the amount of filtered sodium, was decreased in CisPt treated group, due to the reduction in CrCl of these animals. Natriuresis was also lower than control group, as well as reabsorpted sodium, and sodium fractional excretion (NaFE) was increased, indicating that CisPt-treated animals excreted a higher amount of sodium than should be expected when it is relativized to urine/plasma creatinine ratio, due to a decrease in reabsorption process. However, CisPt+5-AIQ group displayed an increased NaTL, which was similar to NaTL of control group. Despite the high value of NaTL, natriuresis and NaFE were decreased in CisPt+5-AIQ group in comparison with control group. NaFE was also decreased when compared with CisPt group. Therefore, CisPt+5-AIQ group displayed increased sodium reabsorption in comparison with CisPt treated group (Table 3).

Strong negative correlation ($p < 0.0001$, $r = -0.9903$) was found between NaFE and CrCl in CisPt treated group (Fig. 2), but no correlation was found in Control ($p = 0.2019$, $r = -0.5049$) or Cispt+5-AIQ ($p = 0.3337$, $r = 0.3943$) groups.

Inhibition of PARP1

14 days after CisPt injection, CisPt-treated rats displayed a significantly higher content of PAR polymer in renal tissue. Treatment with 5-AIQ completely prevented PAR

polymer accumulation (Fig. 3). These results indicate that CisPt treatment enhanced PARP-1 activity, and demonstrate that 5-AIQ is a potent inhibitor of the enzyme.

Renal fibrosis

CisPt group displayed a higher percentage of interstitial fibrosis assessed by Sirius red stain (Fig. 4) 14 days after CisPt injection. 5-AIQ treatment significantly reduced interstitial fibrosis in comparison with CisPt-treated group (Fig. 4).

Renal expression of collagen-IV, α-SMA, and TGF-β1

CisPt group showed a higher expression of some biochemical variables related to fibrosis: collagen-IV, α-SMA, and TGF-β1 (Fig. 5). 5-AIQ treatment completely prevented α-SMA increase (Fig. 6). Collagen-IV and TGF-β1 expressions in CisPt+5-AIQ group were slightly lower than CisPt group, but they did not reach statistical significance (Fig. 5). It is remarkable that the expression of collagen-IV in CisPt+5-AIQ group did not show statistical differences with Control group, indicating that 5-AIQ attenuated collagen expression to an intermediate level between both Control and CisPt groups.

Histopathological analysis

Renal lesions in control group were absent. No glomerular, tubulointerstitial or vascular lesions were present in renal parenchyma. Histopathological examination of renal slices from cisplatin-treated rats showed different alterations, including relevant nuclear dysplasia and incipient acute tubular necrosis (Table 4, Fig. 6). The sections of the kidney from CisPt-treated rats exhibited marked dilation of proximal convoluted tubules in the corticomedullary junction with slogging of almost entire epithelium due to desquamation of tubular epithelium that induced a total absence of microvilli and loss of

brush border in cisplatin group. Also, mild tubular atrophy and apoptotic cells in tubular lumen were present in cisplatin-treated group. CisPt group showed increased interstitial fibrosis in Picro Sirius red and Masson's trichrome staining. 5-AIQ significantly attenuated morphologic alterations induced by cisplatin, indicating that PARP1 activity plays a role in the development of tubular lesions.

Discussion

The main findings of this work are that inhibition of PARP1 with 5-AIQ ameliorates renal dysfunction and prevents body weight loss, decreasing renal fibrosis and tubular lesions in CisPt-treated rats two weeks after treatment. These data for the first time demonstrate that improvements in renal function are maintained during recovery phase of CisPt-induced AKI. Thus, we found that 5-AIQ treatment significantly decreased urinary excretion of NAG, a marker of tubular damage [20], and glucosuria observed in the CisPt group. These last data agree in part with previous reports showing that pharmacological inhibition of PARP1 with PJ34, administered for a shorter period, three [16] or five [7] days after administration of cisplatin, protected against tubular necrosis, renal dysfunction, inflammatory response and oxidative stress. Despite the positive results reported above, we also observed that tubular alterations and renal fibrosis were not completely prevented by 5-AIQ.

In consonance with our results, Kim & Padanilam [21] found that PARP1 deficiency in a model of *Parp1*-KO mice attenuated renal fibrosis and inflammation during unilateral ureteral obstruction, but TGF-β1/Smad3 signaling pathway remained unchanged in *Parp1*-KO and WT mice. In our work, expression of TGF-β1 was also similar in CisPt and CisPt+5-AIQ groups, and this could explain that inhibition of PARP1 did not achieve a complete protection over renal fibrosis and tubular alterations in CisPt

nephrotoxicity. In fact, TGF-β1 was demonstrated to play a role in initiating fibrogenesis in obstructive nephropathy [22], and it has been proposed as the key regulator of renal fibrosis [18].

CisPt is freely filtered at the glomerulus and taken up into renal tubular cells mainly by a transport-mediated process, where it is partially metabolized into toxic species [23]. Hence, CisPt may develop multiple intracellular effects, causing direct cytotoxicity and inducing apoptosis which are not prevented by PARP1 inhibitors in mice [7]. This factor can also contribute to the incomplete protection that we have found in our study.

α-SMA expression was increased in CisPt group, but it was intriguingly reduced to the level of control group in CisPt-AIQ treated rats, although these animals displayed renal fibrosis and high expression of TGF-β1. In this way, it has been recently published that only a minority of collagen-producing cells coexpress α-SMA in the fibrotic kidney, but they were equally capable of activating TGF-β1, suggesting that α-SMA is an inconsistent marker of contractile and collagen-producing fibroblasts in murine experimental models of organ fibrosis [24].

Multiple low doses of CisPt administered during four weeks also induced interstitial fibrosis and increased TGF-β1 and α-SMA expression in mice [25]. In this chronic model, kidney injury and interstitial fibrosis were attenuated by using PXS-4728A, an inhibitor of semicarbazide-sensitive amine oxidase. This antioxidant treatment decreased renal expression of both TGF-β1 and α-SMA in parallel. Besides, these authors observed that blood urea nitrogen and creatinine were decreased in these animals at the end of the study. These results demonstrate that oxidative stress plays a relevant role in CisPt-induced nephrotoxicity. Inhibition of PARP1 has been demonstrated to reduce oxidative stress in acute experiments [7, 16]. Therefore, the

reduction in oxidative stress can also contribute to the improvement in renal function that we have obtained in our study.

Improvement in renal function might be related with sodium handling in these animals. Other authors have described impaired sodium and water transport in CisPt treated rats due to decreased mitochondrial function, decreased ATPase activity and altered cell cation content that alter solute transport [26,27]. Expression of aquaporins and several sodium transporters have been found to be decreased in this model [26,28]. This impaired sodium reabsorption has been related with increased vascular resistance and decreased glomerular filtration rate (GFR) secondary to tubular-glomerular feedback from increased NaCl delivery to the macula densa [27]. According to these findings, in our work we have found a strong negative correlation between NaFE and CrCl in CisPt treated animals, indicating that a higher NaFE is accompanied of a lower GFR in these animals. For the contrary, we have found that 5-AIQ evoked a great increase in sodium reabsorption, probably due to the availability of ATP in renal tubular cells because of the inhibition of PARP1 activity. Increase in sodium reabsorption evoked by 5-AIQ would contribute to normalization of GFR of this group through several mechanisms: for one side, decreased sodium delivery at distal areas of the nephron would inhibit tubular-glomerular feedback increasing GFR and, in the other side, increased sodium reabsorption could determine higher water reabsorption and intake as a homeostatic mechanism aimed to maintain plasma osmolality, increasing filtration fraction and water balance in CisPt+5-AIQ group. The participation of both mechanisms does not exclude the participation of other factors that could increase GFR in CisPt+5-AIQ group. Our data show that correlation between NaFE and GFR is very slight or absent in control and CisPt+5-AIQ groups, indicating that other factors than NaFE contribute to increase GFR in these animals.

Another relevant aspect of this work is that 5-AIQ might be a therapeutic tool in patients that receive CisPt. 5-AIQ has been described as a potent inhibitor of poly(ADP-ribosyl)ation in mice [29]. Although quinolines are generally known as mutagenic and carcinogenic, 5-AIQ does not possess genotoxic activity both in vitro and in vivo systems [30]. Our results demonstrate that 5-AIQ might have a potential therapeutic value to prevent cisplatin nephrotoxicity and the development of fibrosis that has been found to be associated to CisPt treatment [31]. In fact, the second phase of CisPt nephrotoxicity, which is characterized by decreased GFR and impaired NaCl transport does not respond to any drug [32,33], being therefore of clinical interest to evaluate the effects of this substance in other animal models and in patients. Furthermore, these studies should investigate if treatment with 5-AIQ might affect to antitumoral effect of cisplatin.

In summary, this work demonstrates that PARP1 activity participates in the most of nephrotoxic effects evoked by CisPt. The administration of 5-AIQ, a potent PARP1 inhibitor, improves renal function and fibrosis during recovery phase of CisPt-induced AKI in rats. These findings can be of clinical interest to prevent renal dysfunction in CisPt-treated patients.

Acknowledgements

Technical and human support provided by CICT of Universidad de Jaén (UJA, MINECO, Junta de Andalucía, FEDER) is gratefully acknowledged. We also thank the technical assessment of María Dolores Rodríguez.

Author contributions

Conception and design of the experiments: F.O.V., A.O., F.V., R.W. Collection, analysis and interpretation of the data: A.Q., F.O.V., S.M.M., M.G.M., M.C.M., J.F.G., M.C.G., R.W. Drafting the article or revising it critically for important intellectual content: A.Q., F.O.V., S.M.M., M.G.M., M.C.M., J.F.G., M.C.G., A.O., F.V., R.W. All authors approved the final version for publication and agree to be accountable for all aspects of the work in ensuring that questions related to the accuracy or integrity of any part of the work are appropriately investigated and resolved. All persons designated as authors qualify for authorship, and all those who qualify for authorship are listed.

Competing interests

There are no competing interests declared by the authors.

Funding

This study was supported by the grants PI13/02743 and PI13/02384 from the Carlos III Health Institute of Spain, and the Red de Investigación Renal REDinREN RD16/0009/0033. "FEDER una manera de hacer Europa".

REFERENCES

1. Safirstein, R., Winston, J., Moel, D., Dikman, S. and Guttenplan, J. (1987). Cisplatin nephrotoxicity-insights into mechanism. *Int J Androl.* **10**, 325-346

2. Winston, J.A. and Safirstein, R. (1985). Reduced renal blood-flow in early cisplatin-induced acute renal failure in the rat. *Am J Physiol.* **249**, F490-F496

3. Arany, I. and Safirstein, R.L. (2003) Cisplatin nephrotoxicity. *Semin Nephrol.* **23**, 460–464

4. Siddik, Z.H. (2003). Cisplatin: mode of cytotoxic action and molecular basis of resistance. *Oncogene* **22**, 7265–7279

5. Pabla, N. and Dong, Z. (2008). Cisplatin nephrotoxicity: mechanisms and renoprotective strategies. *Kidney Int.* **73**, 994–1007

6. Mukhopadhyay, P., Horváth, B., Kechrid, M., Tanchian, G., Rajesh, M., Naura, A.S. et al. (2011). Poly(ADP-ribose) polymerase-1 is a key mediator of cisplatin-induced kidney inflammation and injury. *Free Radic Biol Med.* **51**, 1774-1788

7. Kim, J., Long, K.E., Tang, K. and Padanilam, B.J. (2012). Poly(ADP-ribose) polymerase 1 activation is required for cisplatin nephrotoxicity. *Kidney Int.* **82**: 193-203

8. Ha, H.C. and Snyder, S.H. (1999). Poly(ADP-ribose) polymerase is a mediator of necrotic cell death by ATP depletion. *Proc Natl Acad Sci USA* **96**, 13978–13982

9. Devalaraja-Narashimha, K. and Padanilam, B.J. (2009). PARP-1 inhibits glycolysis in ischemic kidneys. *J Am Soc Nephrol.* **20**, 95–103

10. Fong, P.C., Boss, D.S., Yap, T.A., Tutt, A., Wu, P., Mergui-Roelvink, M. et al (2009). Inhibition of poly(ADP-ribose) polymerase in tumors from BRCA mutation carriers. *N Engl J Med.* **361**, 123–134

11. Audeh, M.W., Carmichael, J., Penson, R.T., Friedlander, M., Powell, B., Bell-McGuinn, K.M. et al. (2010) Oral poly(ADP-ribose) polymerase inhibitor olaparib

in patients with BRCA1 or BRCA2 mutations and recurrent ovarian cancer: a proof-of-concept trial. *Lancet* **376**, 245–251

12. Fong, P.C., Yap, T.A., Boss, D.S., Carden, C.P., Mergui-Roelvink, M., Gourley, C. et al. (2010). Poly(ADP)-ribose polymerase inhibition: frequent durable responses in BRCA carrier ovarian cancer correlating with platinum-free interval. *J Clin Oncol*. **28**, 2512–2519

13. Drew, Y., Mulligan, E.A., Vong, W.T., Thomas, H.D., Kahn, S., Kyle, S., et al. (2011). Therapeutic potential of poly(ADP-ribose) polymerase inhibitor AG014699 in human cancers with mutated or methylated BRCA1 or BRCA2. *J Natl Cancer Inst.* **103**, 334–346

14. O'Shaughnessy, J., Osborne, C., Pippen, J.E., Yoffe, M., Patt, D., Rocha, C. et al. (2011). Iniparib plus chemotherapy in metastatic triplenegative breast cancer. *N Engl J Med.* **364**, 205–214

15. Hastak, K., Alli, E. and Ford, J.M. (2010). Synergistic chemosensitivity of triple-negative breast cancer cell lines to poly(ADP-ribose) polymerase inhibition, gemcitabine and cisplatin. *Cancer Res.* **70**, 7970–7980

16. Mukhopadhyay, P., Rajesh, M., Cao, Z., Horváth, B., Park, O., Wang, H. et al. (2014). Poly (ADP-ribose) polymerase-1 is a key mediator of liver inflammation and fibrosis. *Hepatology* **59**, 1998-2009

17. Kawai, Y., Satoh, T., Hibi, D., Ohno, Y., Kohda, Y., Miura, K. et al. (2009). The effect of antioxidant on development of fibrosis by cisplatin in rats. *J Pharmacol Sci.* **111**, 433-439

18. Meng, X.M., Nikolic-Paterson, D.J. and Lan, H.Y. (2016). TGF-β: the master regulator of fibrosis. *Nat Rev Nephrol.* **12**, 325-338

19. Sweat, F., Puchtler, H. and Rosenthal, S.I. (1964). Sirius red F3BA as a stain for connective tissue. *Arch Pathol.* **78**, 69-72

20. Bazzi, C., Petrini, C., Rizza, V., Arrigo, G., Napodano, P., Paparella, M. et al. (2002). Urinary N-acetyl-β-glucosaminidase excretion is a marker of tubular cell dysfunction and a predictor of outcome in primary glomerulonephritis. *Nephrol Dial Transplant* **17**, 1890-1896

21. Kim, J. and Padanilam, B.J. (2011). Loss of poly(ADP-ribose) polymerase 1 attenuates renal fibrosis and inflammation during unilateral ureteral obstruction. *Am J Physiol Renal Physiol.* **301**, F450-F459

22. Kaneto, H., Morrissey, J., Klahr, S. (1993). Increased expression of TGF-beta 1 mRNA in the obstructed kidney of rats with unilateral ureteral ligation. *Kidney Int.* 44, 313-321

23. Yao, X., Panichpisal, K., Kurtzman, N. and Nugent, K. (2007). Cisplatin nephrotoxicity: a review. *Am J Med Sci.* **334**, 115-124

24. Sun, K.H., Chang, Y., Reed, N.I. and Sheppard, D. (2016). α-Smooth muscle actin is an inconsistent marker of fibroblasts responsible for force-dependent TGFβ activation or collagen production across multiple models of organ fibrosis. *Am J Physiol Lung Cell Mol Physiol.* **310**, L824-L836

25. Katagiri, D., Hamasaki, Y., Doi, K., Negishi, K., Sugaya, T., Nangaku, M. et al. (2016). Interstitial renal fibrosis due to multiple cisplatin treatments is ameliorated by semicarbazide-sensitive amine oxidase inhibition. *Kidney Int.* **89,** 374-385

26. Daugaard, G. and Abildgaard, U. (1989). Cisplatin nephrotoxicity. A review. *Cancer Chemother Pharmacol.* **25**, 1–9

27. Cornelison, T.L. and Reed, E. (1993). Nephrotoxicity and hydration management for cisplatin, carboplatin, and ormaplatin. *Gynecol Oncol.* **50**, 147–158

28. Lajer, H., Kristensen, M., Hansen, H.H., Nielsen, S., Frøkiaer, J., Ostergaard, L.F. et al. (2005). Magnesium depletion enhances cisplatin-induced nephrotoxicity. *Cancer Chemother Pharmacol.* **56**, 535–542

29. Qian, H., Xu, J., Lalioti, M.D., Gulle, K. and Sakkas, D. (2010). Oocyte numbers in the mouse increase after treatment with 5-aminoisoquinolinone: a potent inhibitor of poly(ADP-ribosyl)ation. *Biol Reprod.* **82**, 1000-1007

30. Vinod, K.R., Chandra, S. and Sharma, S.K. (2010). Evaluation of 5-aminoisoquinoline (5-AIQ), a novel PARP-1 inhibitor for genotoxicity potential in vitro and in vivo. *Toxicol Mech Methods* **20**, 90-95

31. Guinee, D.G. Jr., van Zee, B., Houghton, D.C. (1993) Clinically silent progressive renal tubulointerstitial disease during cisplatin chemotherapy. *Cancer* **71,** 4050–4054

32. Meyer, K.B. and Madias, N.E. (1994). Cisplatin nephrotoxicity. *Miner Electrolyte Metab.* **20**, 201–213

33. Isnard-Bagnis, C. and Deray, G. (2003). Anticancer drugs. In Clinical Nephrotoxins: renal injury from drugs and chemicals, 2nd edn, ed. De Broe, M.E., Porter, G.A., Bennett, W.M. and Verpooten, G.A. pp. 353–372. Kluwer Academic, Dordrecht, Netherlands

FIGURE LEGENDS

Figure 1. Creatinine clearance (CrCl) expressed as ml/min/g of kidney (A) and ml/min/100 g of rat (B) in control, CisPt and CisPt+5-AIQ groups 14 days after CisPt injection. Plasma creatinine (C) and urea (D) concentrations at the end of the experiment in control, CisPt and CisPt+5-AIQ groups. *p<0.001 *vs* control group. +p<0.01, ++p<0.001 *vs* CisPt group (n=8 each group).

Figure 2. Correlation between sodium fractional excretion (NaFE) and creatinine clearance (CrCl) in Control, CisPt and CisPt+5-AIQ groups (n=8 each group) 14 days after CisPt injection.

Figure 3. PAR polymer abundance in renal tissue in control, CisPt and CisPt+5-AIQ groups 14 days after CisPt injection. Results were expressed as percentage of the mean absorbance of the control group. *p<0.001 *vs* control group. +p<0.001 *vs* CisPt group (n=8 each group).

Figure 4. Representative photographs of Picro Sirius red staining of kidneys from control, CisPt and CisPt+5-AIQ-treated rats 14 days after CisPt injection observed with standard light microscopy (top) and the same staining observed with polarized light (down). Bar 50 micrometres (top). Bar 100 micrometres (down). Renal fibrosis (%) quantified with Image J software (right). *p<0.05, **p<0.001 *vs* control group. +p<0.05 *vs* CisPt group (n=8 each group).

Figure 5. Collagen type IV, α-SMA and TGF-β1 expression in renal tissue in control, CisPt and CisPt+5-AIQ groups 14 days after CisPt injection. Results were expressed as percentage of the mean absorbance of the control group. *p<0.05, **p<0.01, ***p<0.001 *vs* control group. +p<0.05 *vs* CisPt group (n=8 each group).

Figure 6. Hematoxylin and eosin (HE, top), Masson's Trichrome (MT, middle) and periodic acid Schiff (PAS) stains in Control, CisPt and CisPt+5-AIQ-treated rats 14 days after CisPt injection. Bar 50 micrometres. Original magnification 20x.

Table 1. Morphologic and metabolic variables determined 14 days after CisPt injection in experimental groups.

	Control	**CisPt**	**CisPt+5-AIQ**
Body weight (g)	272 ± 8.3	240 ± 7.2*	265 ± 6.0
Body weight gain (%)	10.5 ± 0.6	-7.3 ± 0.2***	10.1 ± 0.2^{++}
Kidney weight (mg)	958 ± 49	1210 ± 70*	1099 ± 58
KW/BW (mg/g)	3.51 ± 0.09	5.04 ± 0.25***	4.13 ± 0.15^{+}
Water intake (ml/100g/day)	9.34 ± 0.41	14.5 ± 0.71***	19.9 ± 0.65***,$^{++}$
Diuresis (ml/100g/day)	3.81 ± 0.56	8.51 ± 0.63***	7.25 ± 0.75**
Water balance (ml/100g/day)	5.53 ± 0.29	5.98 ± 0.28	12.7 ± 0.77***,$^{++}$

Data are expressed as means ± SE. *p<0.05, **p<0.01, ***p<0.001 *vs* control group. +p<0.01, ++p<0.001 *vs* CisPt group (n=8 each group). KW/BW: kidney weight/body weight *ratio.*

Table 2. Urinary variables determined in Control, CisPt and CisPt+5-AIQ groups 14 days after CisPt injection.

	Control	**CisPt**	**CisPt+5-AIQ**
Proteinuria (mg/mg creatinine)	1.81 ± 0.22	2.05 ± 0.21	1.54 ± 0.16
Glucosuria (mg/mg creatinine)	0.37 ± 0.06	1.39 ± 0.48*	$0.24 \pm 0.03^{+}$
NAG (mU/mg creatinine)	34.6 ± 5.01	90.5 ± 10.1**	$37.2 \pm 1.98^{++}$

Data are expressed as means ± SE. *p<0.05, **p<0.001 *vs* control grou. +p<0.01, ++p<0.001 *vs* CisPt group (n=8each group). NAG: N-acetyl-β-*D*-glucosaminidase.

Table 3. Sodium handling in Control, CisPt and CisPt+5-AIQ groups 14 days after CisPt injection.

	Control	**CisPt**	**CisPt+5-AIQ**
Plasma Na (mEq/l)	139.7 ± 0.38	142.5 ± 0.55**	140.6 ± 0.45^{+}
NaTL (µEq/min/100g)	61.5 ± 10.2	33.2 ± 10.3**	89.0 ± 6.63^{++}
Natriuresis (µEq/100g/day)	717 ± 75.9	477 ± 20.5*	453 ± 65*
RNa (µEq/min/100g)	61.1 ± 10.1	32.9 ± 10.3**	88.7 ± 6.59^{++}
NaFE (%)	0.86 ±0.09	1.84 ± 0.50*	0.35 ± 0.03*$^{,+}$

Data are expressed as means ± SE. *p<0.05, **p<0.001 *vs* control group. +p<0.01, ++p<0.001 *vs* CisPt group (n=8 each group). NaTL: sodium tubular load; RNa: reabsorpted sodium; NaFE: sodium fractional excretion.

Table 4. Histopathological analysis in Control, CisPt and CisPt+5-AIQ groups 14 days after CisPt injection.

	Control	**CisPt**	**CisPt+5-AIQ**
S3 dysplasia	0	3 (2.5-3)***	1 (1-2)***,++
Acute tubular necrosis	0	2 (2-2)***	1 (1-1.5)**,++
Apoptosis	0	2 (1.5-2.5)***	1 (1-1)***,++
Casts	0	1.5 (1-2)**	0++
Tubular atrophy	0	0	0
Tubular dilation	0	3 (2.5-3)***	1 (1-2)**,++
Vacuolization	0	0	0
Inflammatory infiltrate	0	0 (0-1)	0
Tubular mitosis	0	1 (1-1.5)***	1 (0-1)*,+

Data are expressed as median and interquartilic range. *p<0.05, **p<0.01, ***p<0.001 *vs* control group. +p<0.05, ++p<0.01 *vs* CisPt group (n=8 each group).

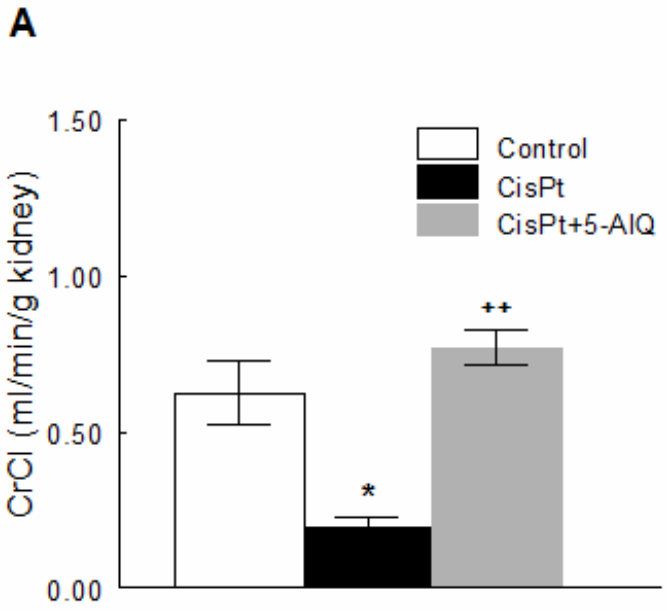
A
1.50
1.00
0.50
0.00
CrCl (ml/min/g kidney)
Control
CisPt
CisPt+5-AIQ
*
++

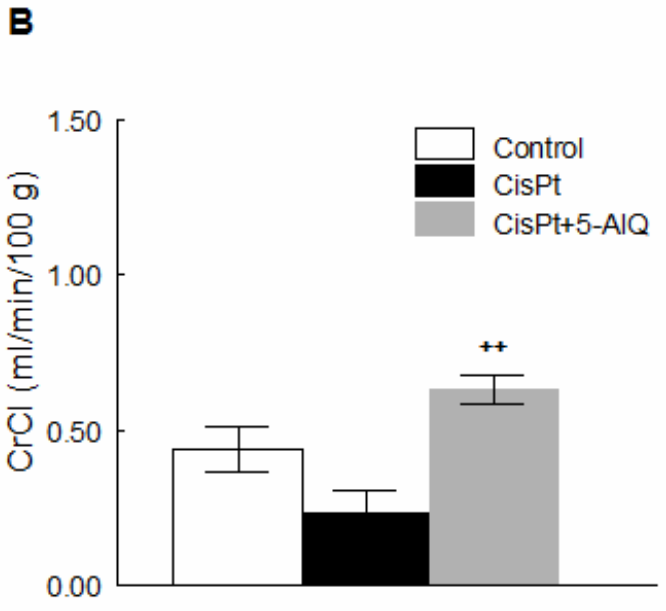
B
1.50
1.00
0.50
0.00
CrCl (ml/min/100 g)
Control
CisPt
CisPt+5-AIQ
++

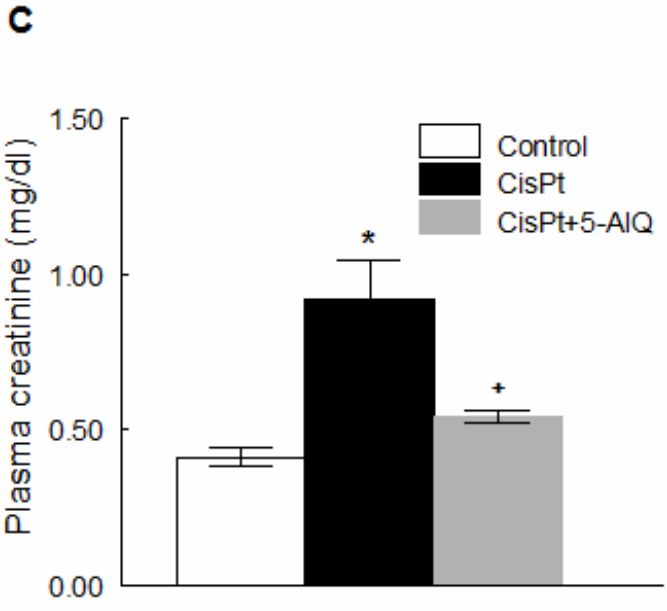
C
1.50
1.00
0.50
0.00
Plasma creatinine (mg/dl)
Control
CisPt
CisPt+5-AIQ
*
+

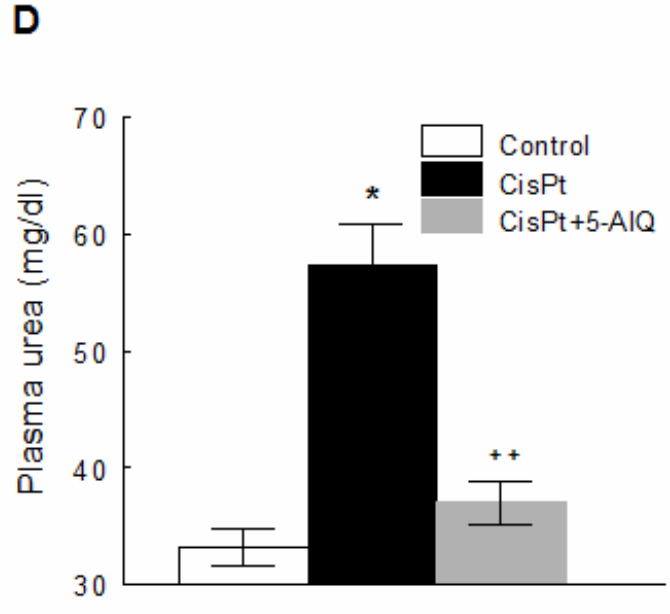
D
70
60
50
40
30
Plasma urea (mg/dl)
Control
CisPt
CisPt+5-AIQ
*
++

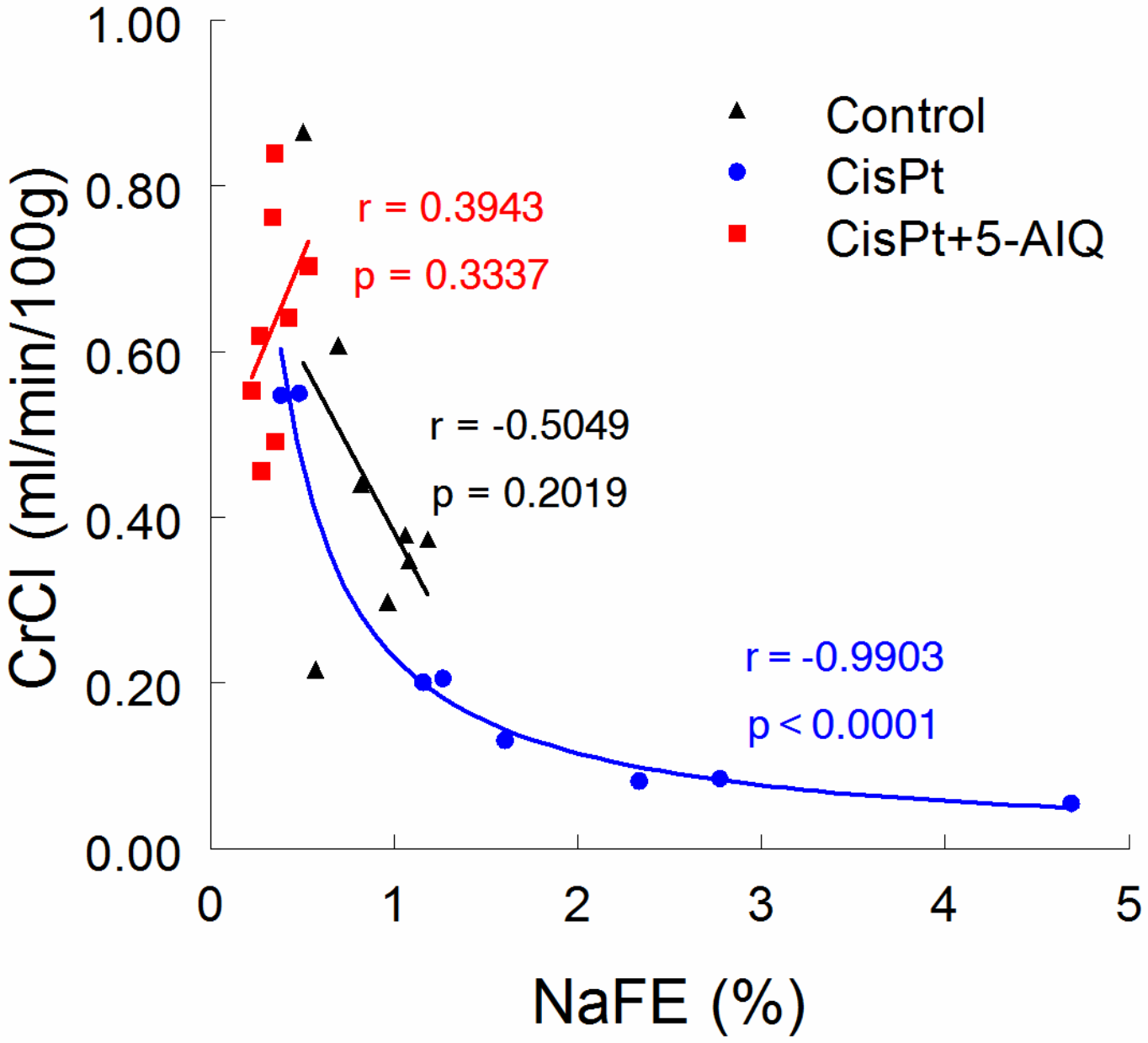
1.00
0.80
0.60
0.40
0.20
0.00
CrCl (ml/min/100g)
0
1
2
3
4
5
NaFE (%)
Control
CisPt
CisPt+5-AIQ
r = 0.3943
p = 0.3337
r = -0.5049
p = 0.2019
r = -0.9903
p < 0.0001

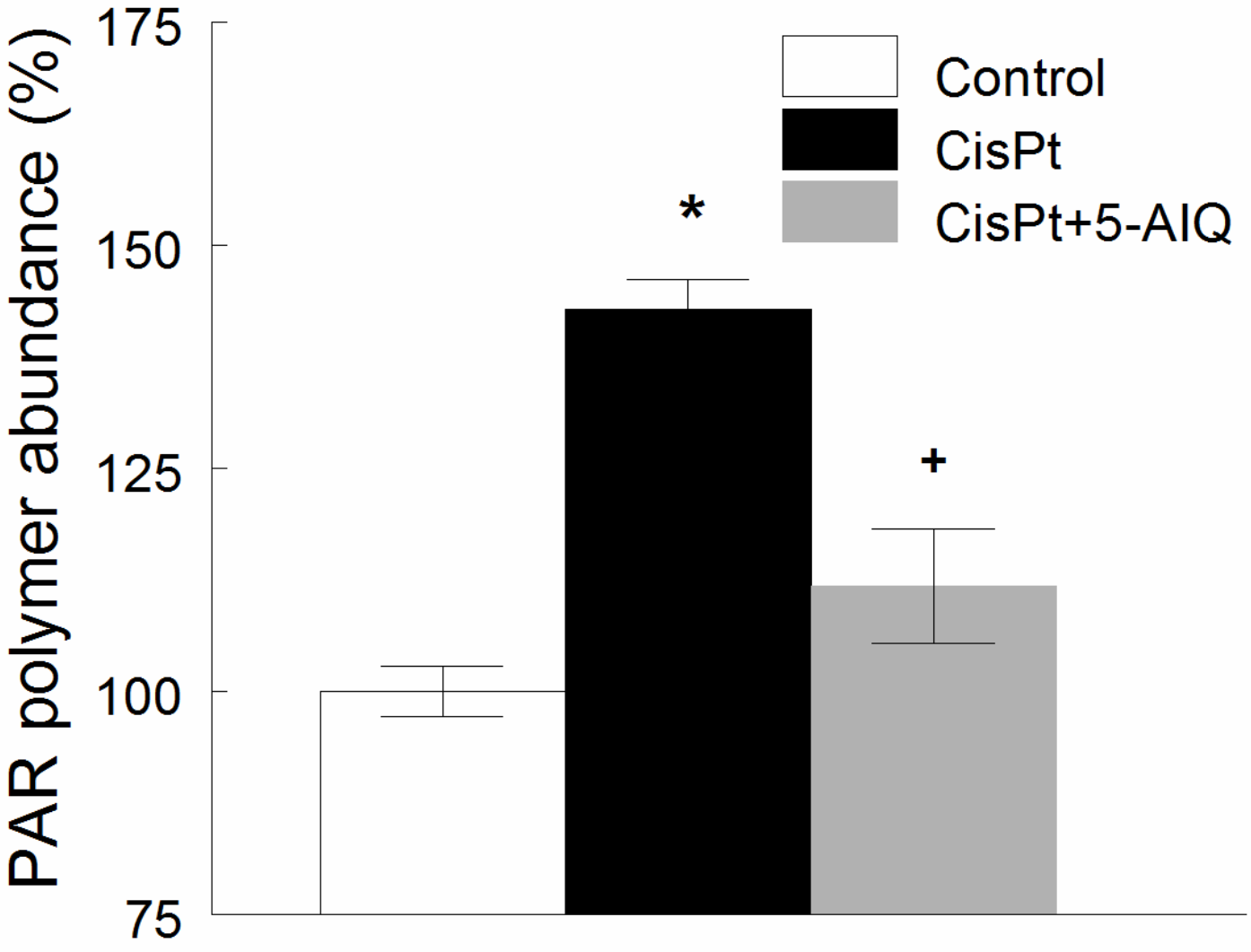
PAR polymer abundance (%)
175
150
125
100
75
Control
CisPt
CisPt+5-AIQ
*
+

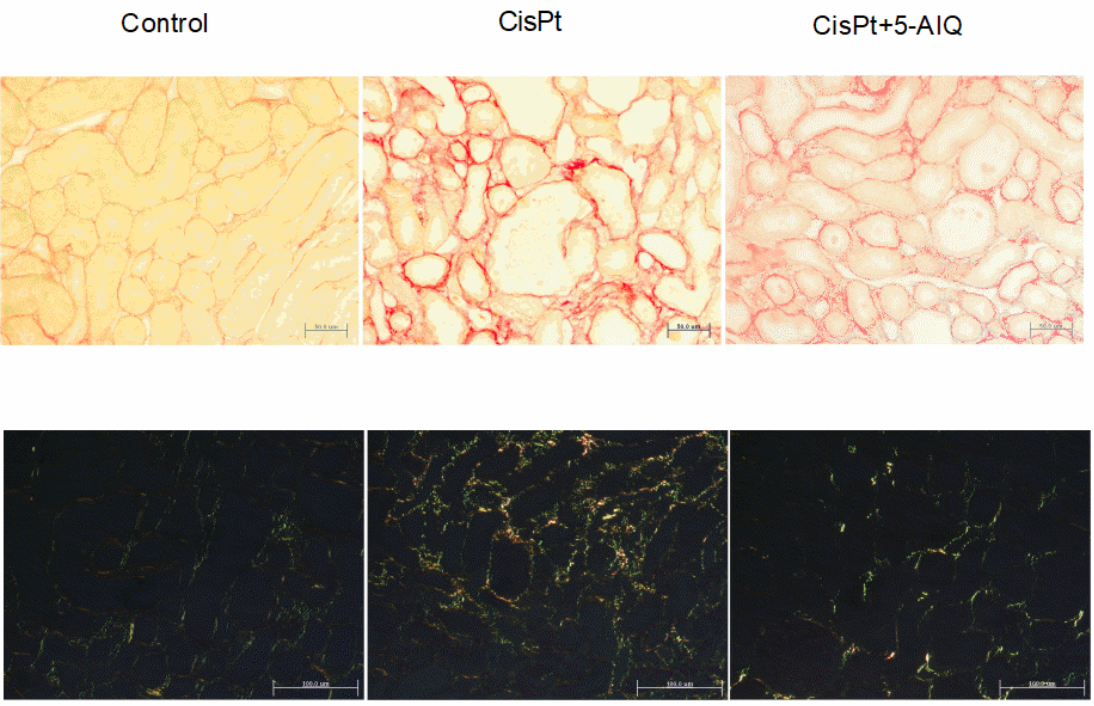
Control
CisPt
CisPt+5-AIQ

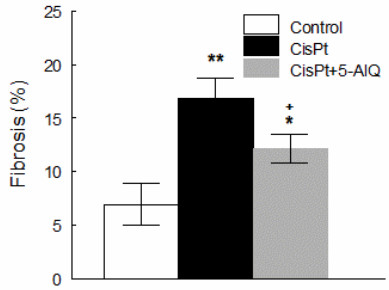
Fibrosis (%)
25
20
15
10
5
0
Control
CisPt
CisPt+5-AIQ
**
+
*

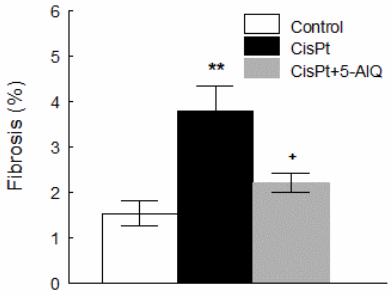
Fibrosis (%)
6
5
4
3
2
1
0
Control
CisPt
CisPt+5-AIQ
**
+

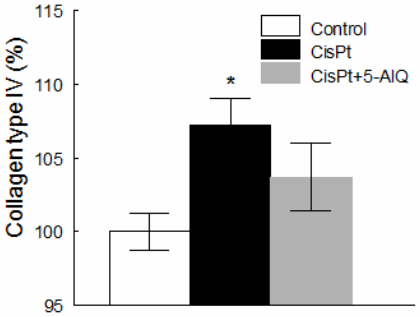
Collagen type IV (%)
115
110
105
100
95
*
Control
CisPt
CisPt+5-AIQ

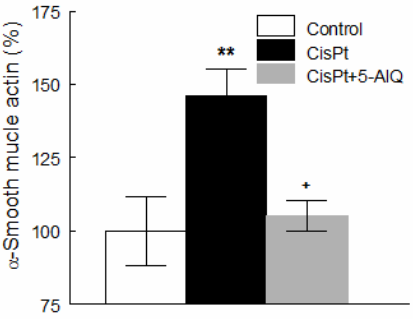
α-Smooth mucle actin (%)
175
150
125
100
75
**
+
Control
CisPt
CisPt+5-AIQ

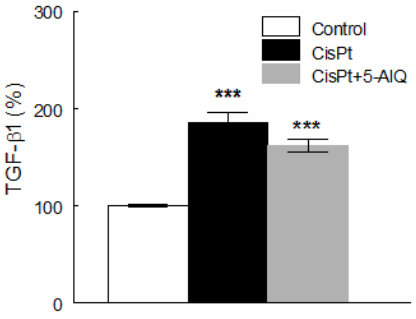
TGF-β1 (%)
300
200
100
0
***
***
Control
CisPt
CisPt+5-AIQ

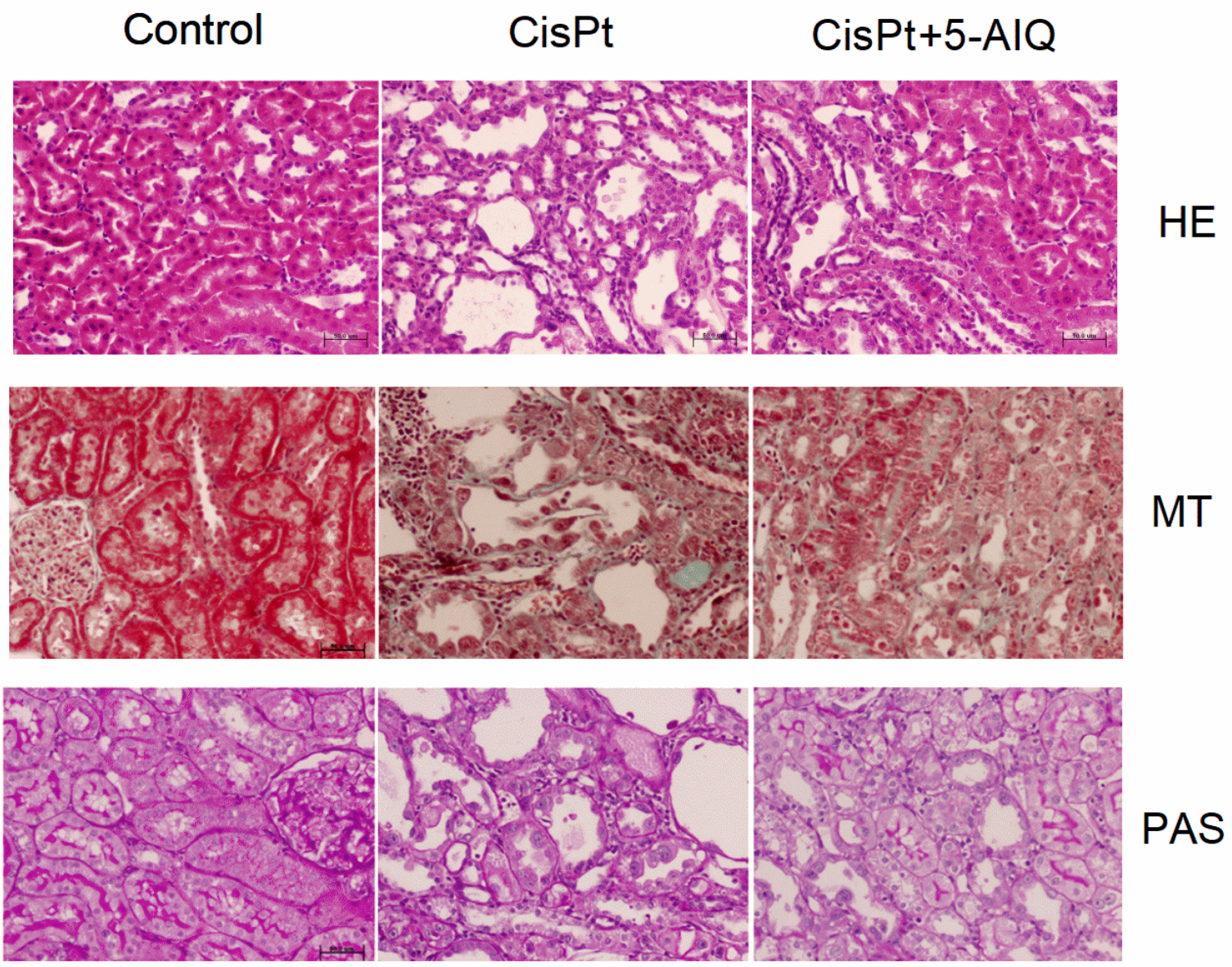
Control
CisPt
CisPt+5-AIQ
HE
MT
PAS